

Formation of Polyamide Nanofibers by Directional Crystallization in Aqueous Solution**

A. Levent Demirel,* Matthias Meyer, and Helmut Schlaad*

Poly(2-alkyl-2-oxazoline)s, which are also referred to as poly(*N*-acyl ethylene imine)s or poly(*N*-acyl aziridine)s (see Figure 1 a), represent an important class of tertiary polyam-

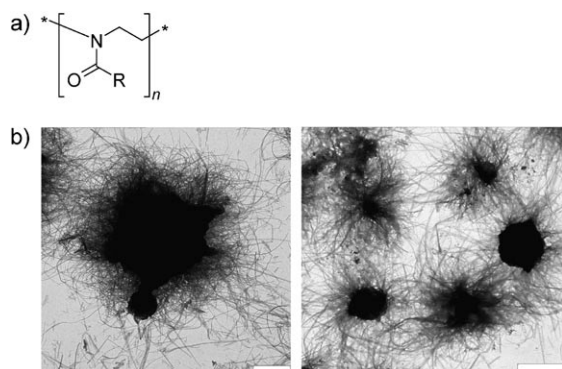


Figure 1. a) Chemical formula of poly(2-alkyl-2-oxazoline). b) Exemplary TEM images of coagulate particles produced by poly(2-isopropyl-2-oxazoline) in pure water (left)^[9] and in a mixture of water and ethylene glycol (95:5 v/v; scale bar: 2 μm).

ides whose properties can be adjusted from amorphous to crystalline and from hydrophilic to hydrophobic depending on the nature of the side chain, R.^[1–4] Oriented filaments were reported to be crystalline in those cases where the alkyl side chains were built of three or more carbon atoms.^[2,3] Polymers carrying methyl, ethyl, propyl, and isopropyl side chains are hydrophilic and soluble in water at temperatures below a lower critical solution temperature (LCST). Poly(2-isopropyl-2-oxazoline) (PIPOX) is the only polymer which is both crystalline and soluble in water (LCST ≥ 30 °C).^[5] Evidently,

PIPOX combines the advantageous properties of two of its structural isomers, that are the crystallinity of polyleucine and the thermoresponsiveness of poly(*N*-isopropylacrylamide) (PNIPAM, LCST ≈ 32 °C). PIPOX may thus be regarded as a thermoresponsive pseudo-peptide.

The operating mechanism leading to the LCST behavior of PIPOX, PNIPAM, and some other acrylamide-based thermoresponsive polymers has been thoroughly investigated.^[6–8] Thermoresponsiveness is the result of dehydration of polymer chains in combination with hydrophobic interactions between alkyl chains, affording a transition of the conformation of a chain from a coil to a globule. The phase transition is usually reversible with hysteresis, but this is not the case for PIPOX if the solution is kept for hours above the LCST. Long-term annealing results in the irreversible formation of micron-sized coagulate particles, which are built of nanofibers (see the transmission electron microscopy (TEM) image in Figure 1 b). Such particles are formed in a self-organization process and not by salting out. PNIPAM does not form any kind of coagulate above the LCST.^[9]

Herein we report, on the basis of scanning force microscopy (SFM), differential scanning calorimetry (DSC), and X-ray diffraction (XRD) studies, that these PIPOX nanofibers are produced through a slow directional crystallization process. The nanofibers ultimately coagulate as micron-sized “balls” with a smaller surface area. The PIPOX sample investigated consisted of an average number of 47 repeat units (polydispersity index of 1.08) and carried a methyl group at the α chain end and two ammonium groups at the ω chain end. The LCST of a 0.05 wt % aqueous solution of PIPOX was 48 °C (as determined by light scattering).^[9]

PIPOX solutions were kept at 65 °C for coagulation. The first coagulate particles were observed in spin-coated films after the solution was kept at 65 °C for approximately 7 h. Figure 2 shows SFM images of a typical PIPOX coagulate in

[*] Prof. A. L. Demirel
Chemistry Department
Koç University
Rumelifeneri Yolu, Sariyer 34450, Istanbul (Turkey)
Fax: (+90) 212–338–1559
E-mail: ldemirel@ku.edu.tr
Dr. M. Meyer, Dr. H. Schlaad
Max Planck Institute of Colloids and Interfaces
Colloid Department
Research Campus Golm, 14424 Potsdam (Germany)
Fax: (+49) 331–567–9502
E-mail: schlaad@mpikg.mpg.de

[**] Irina Shekova, Markus Antonietti, and Erich C. are thanked for their contributions to this work. This work was funded by the Max Planck Society.

Supporting information for this article is available on the WWW under <http://www.angewandte.org> or from the author.

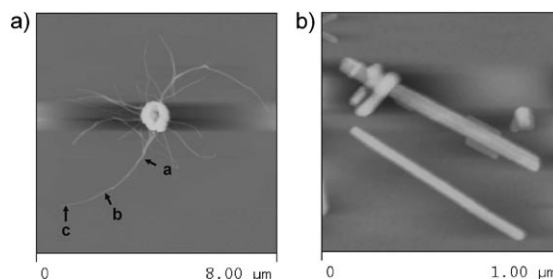


Figure 2. a) SFM height picture of a typical nanofiber containing PIPOX coagulate formed in water at 65 °C after 7 h (see text for details about spots a, b, and c). b) Close-up height picture of the nanoribbons that form the nanofibers.

the early stages of structure formation. It has a central core from which nanofibers emanate. These nanofibers are thicker and wider closer to the core, and the dimensions decrease towards the tips. For instance, the lower left nanofiber shown in Figure 2a exhibits a height/width ratio of 34:90 nm close to the core (spot a); 21:79 nm in the middle of the fiber (spot b), and only 15:57 nm at the tip (spot c). The building blocks for these nanofibers are actually nanoribbons that have a well-defined rectangular prismatic shape. A small segment of two of these nanoribbons is shown in the SFM image in Figure 2b. The height of both ribbons is 15 nm, but the width of the upper is approximately 70 nm and that of the lower is approximately 43 nm. A brighter region with a slightly larger thickness is visible in the middle of the upper nanoribbon. This suggests that the nanoribbon building blocks can fuse together to result in thicker and wider nanoribbons, which eventually turn into nanofibers. Their length can be up to several microns.

The crystallinity of dried PIPOX coagulate, formed in water at 65 °C within 24 h, was confirmed by DSC and XRD measurements. In the first DSC heating scan (see Figure 3a), two endothermic peaks occur at 178 °C (minor) and 195 °C (major), attributable to the melting of the sample. The intensity of the melting peak(s) decreased in subsequent heating scans possibly as a result of thermal damage of the polyamide at higher temperatures; the glass transition of PIPOX was found to occur at around 70 °C (see Supporting Information). A very similar heating curve was found for PIPOX after isothermal crystallization at 130 °C (performed in the DSC instrument). Endothermic peaks had maxima at 177 °C and 198 °C.

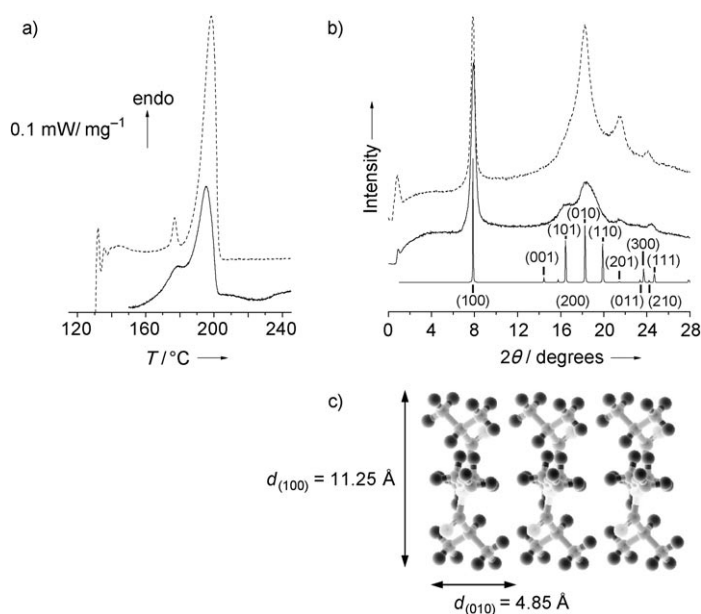


Figure 3. a) DSC first-cycle heating curves and b) XRD data of isothermally crystallized PIPOX at 130 °C (dashed lines) and of dried PIPOX coagulate formed in water at 65 °C (solid lines). The calculated peak positions, peak intensities, and indexing are seen below the experimental data and correspond to the crystal structure shown in part (c).

In XRD, the latter samples showed two major peaks at $2\theta = 7.85^\circ$ ($d = 11.25 \text{ \AA}$) and 18.25° (4.85 \AA); two smaller peaks also appeared at 21.50° (4.13 \AA) and 24.00° (3.70 \AA). These four peaks with varying intensities were also observed in the XRD data of PIPOX coagulate, together with a shoulder at 16.3° (5.43 \AA). Observation of identical endothermic peaks in the DSC scans and the same crystalline peaks in XRD for both coagulated PIPOX and isothermally crystallized PIPOX confirms that the structure formation in aqueous solution above the LCST is also a crystallization process. The amorphous parts seen in DSC and XRD data are attributed to the presence of non-crystallized PIPOX molecules, which were also evident as a smooth film in spin-coated samples.

The model crystal structure seen in Figure 3c (see also the Supporting Information) captures the experimentally observed XRD peaks. The polymer backbones are aligned along the [001] direction, that is, perpendicular to the plane of the structure in Figure 3c. The isopropyl side groups are alternately aligned along the [100] direction to either side of the backbone. Thus, the amide dipoles are oriented along the [010] direction, also alternating in direction.

The model structure in Figure 3c together with the SFM structural characterization contribute to the understanding of the self-organization of PIPOX in solution into directionally crystallized nanoribbons. The period along the backbone of a stretched PIPOX chain (-NCCNCC-) that has an all-*trans* configuration is 7.6 \AA . Experimentally, the periodicity was found to be 6.4 \AA ,^[2] with the shorter distance being attributable to rotation around C–C bonds, which is consistent with our model in Figure 3c. The average contour length of PIPOX chains consisting of an average of 47 repeat units is approximately 15 nm, which corresponds to the thickness of nanoribbons as measured by SFM. Seemingly, in the ribbons, the chains are fully stretched and not folded. The [001] direction of the nanoribbons is thus determined by the backbone length. The observation of both (100) and (010) peaks in XRD indicates an enhanced fusion of nanoribbons in the dried coagulate similar to that seen in Figure 2b. To prevent the fusion of nanoribbons, we added 2–5 vol % ethylene glycol to the aqueous solutions. The polymer coagulated as before into nanofiber-containing particles (see Figure 1b), but the (100) peak was absent in the XRD profile of the dried coagulate (see Supporting Information). Nanoribbons were thus growing faster along the [010] direction than along the [100] direction.

The morphology of the coagulate in solution and in spin-coated films could be controlled by varying the processing conditions. Formation of spherical particles was hindered and a mesh of nanofibers was obtained by the addition of tetrahydrofuran as a cosolvent (ca. 2 vol %) and vigorous stirring (see Figure 4 as well as the Supporting Information). Note that the cosolvent evaporates completely during the process of coagulation.

The non-specific hydrophobic interactions^[10] by themselves cannot explain the observed anisotropic structures of PIPOX. PNIPAM also separates into two phases above the LCST, as a result of similar non-specific

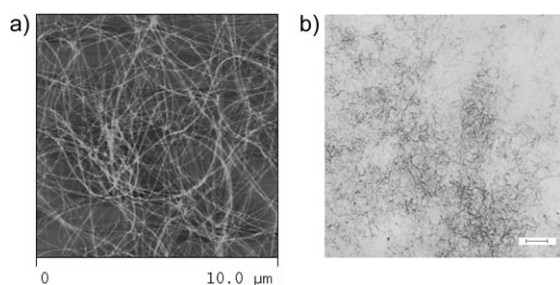


Figure 4. a) SFM height picture and b) optical micrograph (scale bar: 10 μm) of the PIPOX coagulate formed under stirring in a mixture of water and tetrahydrofuran (98:2 v/v) within 24 h at 65 °C.

hydrophobic interactions, without producing coagulate. Specific hydrogen-bonding interactions,^[11] on the other hand, could be ruled out on the basis of infrared (FTIR) spectroscopy measurements (see Supporting Information). To account for the observed directional crystallization, we propose a mechanism that involves both non-specific hydrophobic interactions and oriented dipolar interactions. Non-specific hydrophobic interactions bring the isopropyl side groups of PIPOX together in the aqueous medium. This allows the amide dipoles of the PIPOX to interact and align. The direction of the fastest crystallization ([010] direction in Figure 3c) is determined by the orientation of the dipoles. The chains are then packed such that the dipoles are aligned, causing dominant anisotropic growth along the [010] direction. In addition to the thermodynamics of structure formation, the amide dipole $\text{N}^+=\text{C}-\text{O}^-$ plays an important role in the crystallization kinetics of PIPOX, as one end of the dipole (N^+) is on the polymer backbone (not so in PNIPAM). Solvation of the PIPOX dipoles increases the mobility of the polymer backbones. Without this “plasticizing effect”, PIPOX would not crystallize at 65 °C, which is below the bulk glass transition temperature (ca. 70 °C). An increased backbone mobility is also essential in promoting equilibration of the system, thus leading to the formation of very regular nanofibers with smooth edges and well-defined dimensions (as seen in Figure 2b).

In summary, we report that PIPOX, which may be regarded as a thermoresponsive pseudopeptide, undergoes a directional crystallization into nanoribbons in aqueous solution above its LCST as a result of hydrophobic and dipolar interactions. Solvation appears to be especially important in lowering the kinetic barriers in the crystallization process, similar to the self-organization of polypeptides and proteins.

Experimental Section

Descriptions of experimental procedures and analytical methods and instrumentation are provided in the Supporting Information.

Received: August 1, 2007

Published online: October 1, 2007

Keywords: colloids · crystal growth · hydrophobic effect · nanostructures · polymers

- [1] T. G. Bassiri, A. Levy, M. Litt, *J. Polym. Sci. Part B* **1967**, 5, 871–879.
- [2] M. Litt, F. Rahl, L. G. Roldan, *J. Polym. Sci. Polym. Phys. Ed.* **1969**, 7, 463–473.
- [3] R. Hoogenboom, M. W. M. Fijten, H. M. L. Thijs, B. M. van Lankvelt, U. S. Schubert, *Des. Monomers Polym.* **2005**, 8, 659–671.
- [4] F. Wiesbrock, R. Hoogenboom, M. Leenen, S. F. G. M. van Nispen, M. van der Loop, C. H. Abeln, A. M. J. van den Berg, U. S. Schubert, *Macromolecules* **2005**, 38, 7957–7966.
- [5] J.-S. Park, Y. Akiyama, F. M. Winnik, K. Kataoka, *Macromolecules* **2004**, 37, 6786–6792.
- [6] C. Diab, Y. Akiyama, K. Kataoka, F. M. Winnik, *Macromolecules* **2004**, 37, 2556–2562.
- [7] Y. Maeda, T. Higuchi, I. Ikeda, *Langmuir* **2000**, 16, 7503–7509.
- [8] Y. Maeda, T. Nakamura, I. Ikeda, *Macromolecules* **2001**, 34, 8246–8251.
- [9] M. Meyer, M. Antonietti, H. Schlaad, *Soft Matter* **2007**, 3, 430–431.
- [10] D. Chandler, *Nature* **2005**, 437, 640–647.
- [11] J. T. Meijer, M. Roeters, V. Viola, D. W. P. M. Löwik, G. Vriend, J. C. M. van Hest, *Langmuir* **2007**, 23, 2058–2063.